Spermidine Mitigates Immune Cell Senescence, Enhances Autophagy, and Boosts Vaccine Responses in Healthy Older Adults.

Ghada Alsaleh

Ghada.Alsaleh@ndorms.ox.ac.uk

Botnar Institute for Musculoskeletal Sciences, Nuffield Department of Orthopaedics, Rheumatology and Musculoskeletal Sciences, University of Oxford https://orcid.org/0000-0002-4211-3420

Mohammad Ali

Peter Medawar Building for Pathogen Research, Nuffield Department of Clinical Medicine, University of Oxford

Amir Kayvanjoo

Max-Delbrück Center for Molecular Medicine in the Helmholtz Association, Berlin, Germany https://orcid.org/0000-0003-1315-8336

Feng Liu

Botnar Institute for Musculoskeletal Sciences, Nuffield Department of Orthopaedics, Rheumatology and Musculoskeletal Sciences, University of Oxford.

Sagida Bibi

CAMS-Oxford Institute, Nuffield Department of Medicine, University of Oxford.

Lin Luo

Kennedy Institute of Rheumatology, University of Oxford.

Melissa Govender

Centre for Human Genetics and the Pandemic Sciences Institute, Nuffield Department of Medicine, University of Oxford

Miles Carroll

Centre for Human Genetics and the Pandemic Sciences Institute, Nuffield Department of Medicine, University of Oxford

Sebastian Hofer

Max Delbrück Center Berlin https://orcid.org/0000-0002-0756-0014

Tobias Eisenberg

University of Graz https://orcid.org/0000-0003-3559-1130

Christoph Magnes

HEALTH - Institute for Biomedical Research and Technologies, Joanneum Research Forschungsgesellschaft

Loren Kell
University of Oxford https://orcid.org/0000-0003-1322-2027
Christopher Chung
Botnar Institute for Musculoskeletal Sciences, Nuffield Department of Orthopaedics, Rheumatology and Musculoskeletal Sciences, University of Oxford
Yu Deng
Botnar Institute for Musculoskeletal Sciences, Nuffield Department of Orthopaedics, Rheumatology and Musculoskeletal Sciences, University of Oxford
Aneesha Bhandari
Centre for Global Health Research, Nuffield Department of Clinical Medicine, University of Oxford
Liye Chen
Botnar Institute for Musculoskeletal Sciences, Nuffield Department of Orthopaedics, Rheumatology and Musculoskeletal Sciences, University of Oxford
Barbara Kronsteiner-Dobramysl
Peter Medawar Building for Pathogen Research, Nuffield Department of Clinical Medicine, University of Oxford
Susie Dunachie
Peter Medawar Building for Pathogen Research, Nuffield Department of Clinical Medicine, University of Oxford
Owen Spiller
Department of Microbiology, University Hospital of Wales, Heath Park, Cardiff University
Teresa Lambe
CAMS-Oxford Institute, Nuffield Department of Medicine, University of Oxford, Oxford, UK
Paul Klenerman
Centre for Global Health Research, Nuffield Department of Clinical Medicine, University of Oxford, Oxford
Lucy Jones
Department of Microbiology, University Hospital of Wales, Heath Park, Cardiff University
Anna Katharina Simon
Max Delbrück Center for Moleculare Medicine (MDC)

Article

Keywords:

Posted Date: April 2nd, 2025

DOI: https://doi.org/10.21203/rs.3.rs-5686388/v1

Additional Declarations: Yes there is potential Competing Interest. A.K.S. and T.E. are consultants for TLL The Longevity Labs GmbH and Oxford Healthspan. G.A. is a consultant for Oxford Healthspan. TLL had no input into the trial design, results, analysis, or manuscript.

Abstract

Older adults are particularly vulnerable to infectious diseases, and vaccines are often less effective in this population due to immunosenescence, which is characterized by diminished B and T memory responses. Autophagy is believed to underlie many facets of cellular aging, including immunosenescence. It is crucial for maintaining memory T and B cell functions but declines with age, along with the endogenous metabolite spermidine that helps maintain autophagy levels. We conducted a double-blind, randomized, placebo-controlled study in 40 volunteers over 65, administering oral spermidine after their third SARS-CoV-2 vaccine dose. Spermidine reduced immune cell senescence, evidenced by decreased p16 expression in lymphocytes. Following spermidine treatment, autophagic flux, TFEB targets, and autophagy-related genes detected by scRNA-seq were highly enriched in B cells. Spermidine significantly increased spike-specific IgG secretion and memory B cells, and neutralizing antibody activity against SARS-CoV-2 strains, in vaccine non-responders that also presented with high immune cell senescence. Targeting immune senescence using spermidine may offer a practical approach to improve immune responses in vaccine non-responders, as a post- or pre-vaccination intervention. Additionally, it highlights the utility of immune senescence markers as predictive biomarkers for identifying vaccine non-responders, addressing a key challenge in vaccine development for an aging population.

Introduction

Enhancing immune resilience to existing and emerging infections is key to improving the healthspan of older adults. Impaired immune responses and “inflammaging” (chronic, low-grade inflammation) contribute to age-related health issues[1]. Collectively, the age-related gradual dysfunction of the immune system is termed immunosenescence[2], which, along with comorbidities, genetics and environmental factors, weaken vaccine responses. During the SARS-CoV-2 pandemic over 92% of deaths occurred in people aged over 60[3]. Vaccination programmes have been central to the prevention of infection-associated morbidity and mortality. However, vaccines often work less effectively in older adults and protective immune responses can be hard to achieve in this vulnerable group[4–7], as indicated by reduced amplitude and duration of both immune responses, for example, to hepatitis A and B[8–10], trivalent influenza (TIV)[11–13], and tick-borne encephalitis (TBE)[14]. Similarly, lower neutralizing antibody levels against SARS-CoV-2 were observed in individuals over 80, regardless of vaccine platform[15,16]. Furthermore, older adults also have lower T cell vaccine responses[11–13,17,18]. While mRNA and ChAdOx vaccines against SARS-CoV-2 have been effective in older adults[19], vaccine non-responders were observed, especially those with comorbidities such as obesity[20]. To tackle poor vaccine responses in older adults, targeting immunosenescence may offer a more practical approach than developing novel vaccines for different age groups for each pathogen[21]. Identifying a biomarker for vaccine non-responders could also help target this population. Key to improving immune resilience in older adults is

reducing the "cellular age" of immune cells. This includes addressing issues like replicative senescence, poor mitochondrial health, dysregulated nutrient sensing and poor protein quality control mechanisms[22].

One cellular process that is a promising target is autophagy, which is essential for immune function[23,24]. Autophagy is responsible for the control of protein quality, and the regulated breakdown and recycling of damaged cellular components, but declines with age. Compromised autophagy has been deemed an indicator of progressed aging[25] across species[26–29]. While upregulation of autophagy genes extends organismal lifespan[30–32], conversely, deletion of key autophagy genes in mice leads to premature aging of the immune system, with loss of numbers or function of hematopoietic stem cells[33], macrophages[34] and memory $CD8^+$ T cells[35,36]. We have also previously observed an age-related decline of autophagic flux in human peripheral $CD8^+$ T cells[29,37], which correlates with poorer vaccine responses. Importantly, we have demonstrated that supplementing aged mice with the endogenous metabolite spermidine improves $CD8^+$ T and B cell memory responses[36,38]. Based on these concepts, we set out to conduct the first clinical study in humans that specifically targets autophagic function to improve immunosenescence and elevate vaccine responses in older adults.

Spermidine, a compound found in foods like wheat germ, has shown promise in improving autophagy in mice[36,38]. Research has demonstrated that spermidine can enhance autophagy in immune cells, particularly in T[29] and B cells[38]. Our studies and others have shown that spermidine enhances immune cell function by hypusinating eukaryotic translation initiation factor 5A (eIF5A), which in turn facilitates the translation of proteins with challenging motifs, such as polyprolines, and mitochondrial proteins[38,39]. In B cells, eIF5A supports the translation of transcription factor EB (TFEB), a key regulator of lysosomal biogenesis and autophagy, and is also necessary for the synthesis of the autophagy-related protein Atg3[38,40].

To test the effects of spermidine on immune function in older adults, a double-blind, randomized study was conducted. Twenty participants over the age of 65 received 6 mg of spermidine daily, while another 20 received a placebo following their third SARS-CoV-2 vaccination. The study measured immune responses, including spike-specific IgG levels, memory B cell responses, antibody inhibition of spike-ACE2 receptor binding, autophagy levels and cellular senescence.

Our study, despite its small size, demonstrates that spermidine significantly improved vaccine responses in the treatment group. More importantly, it highlights the potential for enhancing vaccination strategies in older adults by identifying vaccine non-responders through screening for senescence markers.

Results

Study design and baseline demographics

To test whether the autophagy-inducing compound spermidine improves immune memory responses in humans, we set up a double-blinded, randomized, placebo-controlled experimental medicine study with

40 adults over 65 years of age. The 40 volunteers had been vaccinated three times prior to this study as part of the UK's national SARS-CoV-2 vaccine roll-out. As it is known that anti-spike IgG responses peak in the first week after the 3rd dose, the dietary intervention was started at least 1 week, and at most 8 weeks, after the last immunization (Fig. S1A, B). Blood samples were taken at baseline (before spermidine administration), and at 2 and 13 weeks after spermidine initiation. After a wash-out period of 24 weeks without any spermidine or placebo administration, final blood samples were taken at 37 weeks.

Clinical safety of the nutraceutical

Our primary endpoint was the safety of a daily oral spermidine supplement for 13 weeks, after triple SAR-CoV-2 vaccination. In the placebo group, 9 participants were female (50%) and 9 were male (50%), whilst in the spermidine group 13 participants were female (75%) and 7 were male (35%). All participants were White British. Baseline characteristics were similar between groups (Table 1). At week 0 (baseline) there were no participants in the placebo or spermidine groups with a history of COVID-19 like illness or SARS-CoV-2 positive rt-PCR diagnosis (Table 1).

Spermidine supplementation rejuvenated senescent cells and enhanced vaccine responses.

We first assessed whether serum IgG against the spike protein could inhibit the binding of the spike protein to Angiotensin-Converting Enzyme 2 (ACE2), the entry receptor for SARS-CoV-2, using a pseudo-neutralizing antibody assay. Notably, spermidine significantly enhanced the blocking antibody response to the spike protein from most viral strains at 2 weeks compared to baseline (Fig. 1A). Next, we measured serum anti-spike IgG levels by ELISA. Interestingly, while spermidine treatment increased anti-spike IgG levels at 2, 13, and even 37 weeks, the effect was not statistically significant (Fig. 1B). Similar effects were observed in spike-specific memory B cells, as shown by FluoroSpot assays that measured IgG-secreting cells (Fig. 1C,D). An important observation from the data showed that only certain participants improved their vaccine response after spermidine supplementation, while others did not. Interestingly, none of the obvious factors such as age, BMI, gender, vaccine type, or time since vaccination could explain this difference (Figure 1B and Table 1 and 2). The only notable distinction was the same subgroup of 8 participants who were vaccine non-responders receiving spermidine (Group 2, 'G2') (Fig. 2A), displayed very low to undetectable antibody titres (below threshold indicated on graph = seronegative) and elevated levels of key cellular senescence markers, including p16 (*CDKN2A*), γ-H2AX (a DNA damage marker), and phosphorylated S6 (pS6, a downstream target of mTORC1 activity) at baseline (Fig. 2B-D). Remarkably, spermidine treatment reduced pS6 and p16 levels after two weeks in all participants taking spermidine in both seropositives (G1) and seronegatives (G2) suggesting decreased immune cell senescence (Fig. 2E,F). On the other hand, γ-H2AX levels did not show any significant changes after spermidine treatment (Fig. 2G). Notably, although p21 (CDKN1A), another cellular senescence marker, appeared to be elevated in G2, was neither significantly increased nor altered by spermidine supplementation in G2 (Fig. S2A,B) . Interestingly, all 8 participants that were initially seronegative (G2) showed a remarkable increase in antibody titres, rising from 377.42 (± 268.76)

to 28,331.02 (± 23,976.87), representing an average 75-fold increase after just two weeks of spermidine (Fig. 3A and Fig. S2C). This significant rise in IgG titres was sustained at 13 weeks (Fig. 3B) and persisted at 37 weeks, even after the 24-week washout period (Fig. 3C). In contrast, the remaining 12 participants who were seropositive at baseline receiving spermidine (G1) with a low expression of senescence markers (Fig. 2B-D) had mean IgG titres of 18,011 (± 10,307.33), and showed no significant change after spermidine 16,240.5 (± 10,570.70) (Fig. 3A-C and Fig. S2C). The placebo group, including seronegative and seropositive at baseline also did not exhibit this increase (Fig. 3A-C and Fig. S2C), suggesting that spermidine may enhance long-term antibody titres by either improving cellular immune responses or promoting the persistence of immunoglobulins in the serum.

Additionally, G2 exhibited a significant rise in IgG-secreting memory B cells at week 2 (Fig. 3D). As previously, at baseline G2 as opposed to G1 mounted very weak responses (Fig. S2D). G2 treated with spermidine showed a large increase in IgG-secreting memory cells at week 2 in IgG-secreting memory cells (Fig. 3D and S2D). Notably, the proportion of total memory B cells in blood, identified by CD27 and IgD, was unchanged in flow cytometric analysis (Fig. S2E) and spermidine did not affect total IgA or IgG in this assay (Fig. S2F-H). Together, this indicates that spermidine improves the vaccine-specific antibody-secreting function of memory B cells, rather than the half-life of immunoglobulins. Notably, when we now divided the group into G1 and G2 and assessed the inhibition capacity of serum IgG directed against the spike protein using our pseudo-neutralising antibody assay, we observed similar results to those obtained via ELISA (Fig. 2A). Specifically, G2 exhibited a weak inhibition response at baseline. However, after 2 or 13 weeks of spermidine treatment, the absolute levels of serum IgG against most tested SARS-CoV-2 strains significantly increased in this group (Fig. 3E and S3A-I).

We then probed whether anti-SARS-CoV-2 T cell responses were also improved in the spermidine-treated group. IFN-g in ELISpots of whole PBMCs after re-stimulation with SARS-CoV-2 peptide pools (S1, S2) revealed no differences between placebo and spermidine groups, neither when comparing week 0/baseline with spermidine treatment (fold-change) within individuals nor when dividing groups by IgG titres at baseline (G1 and G2, Fig. S4A-D).

Spermidine treatment alters B cell pathways

To shed light on this and the molecular differences between seropositive and seronegative individuals, we performed single-cell RNA sequencing (scRNA-seq) on samples from 5 vaccinees in each group (placebo, spermidine G1 and G2) at week 0 and week 2. Our cluster analysis successfully identified all anticipated PBMC subsets by utilizing reference mapping from a comprehensive multimodal PBMC reference dataset provided by Seurat[41] (Fig. 3F). To ensure the accuracy of our findings, we manually reviewed the clusters identified through this mapping process (Supplementary Fig. S5A).

In line with the outcome of our analyses of lymphocyte function, we observed the most significant changes in B cells. Expression analysis identified a considerable number of differentially expressed genes (DEGs) in both memory and naïve B cells when analysed across all groups (Fig. 3G-H). Interestingly, BCR activation stood out from several significantly changed annotated biological

processes, including regulation of autophagy and the ER stress pathway in both naïve and memory B cells (Fig. 3G-H). Transcripts related to inflammation were also significantly changed from week 0 to week 2 (Fig. 3G-H). In addition to these biological processes, we found senescence (cell cycle and DNA repair) and metabolism pathways changed in naïve B cells at week 2 (Fig. 3G-H).

Dissecting these pathways, we found that transcripts for positive regulators of BCR signalling/differentiation/survival were significantly increased only in seronegative individuals receiving spermidine (G2) between baseline and 2 weeks of spermidine treatment. These included *CD27*, *LYN*, *XBP1*, *EZR*, and *IL4R* in memory B cells (Fig. 3I) and *BCL10, BTK, THEMIS2, Ly9, RHOH,* and *BACH1* in naïve B cells (Fig. 3K). In line with this, negative regulators of BCR signalling were downregulated by spermidine in G2, such as *LAT2, PTPN6, SLAMF6*, and *SH2B2* (Fig. 3I-K). Interestingly, typical autophagy transcripts were significantly upregulated in G2 only, including *ATG14, ATG9* and others including *BAG3, ULK3, SNX18, NRBF2, RIPK2* (Fig. 3I-K). Most intriguingly, we found a signature of reduced senescence with induced cell cycle and DNA repair genes in naïve and memory B cells (e.g. *DBF4, AKAP8, PIK3CA, JMY, EZH2* and *SIRT2*) and decreased transcripts encoding proteins that limit cell cycle (e.g. *ING4, CDKN2D* encodingp19) (Fig. 3I-K). Interestingly, we noticed in G2 that memory B cells at baseline have increased expression of *FCER2* (also known as CD23) and decreased expression of *TNFRSF13B* (also known as TACI) compared to G1 and placebo baseline (Fig. S5B-C). This indicates that memory B cells in G2 may have an altered threshold for activation. Furthermore, *SLC18B1*, a polyamine transporter, shows higher expression at baseline in memory B cells from G2 compared to G1 and placebo groups (Fig. S5D). This suggests that these memory B cells in G2 may have a higher demand for spermidine (Spd), making them more primed for autophagy. In addition, we observed differences relevant to the innate immune response between G2 and G1 in B cells (Fig. S5E-D). All gene transcripts in the biological process category that characterise TLR and TLR signalling pathways behaved quite differently even at baseline between placebo/G1 and G2, and were uniformly downregulated with spermidine in G2 volunteers (*TLR7, TLR9, TLR10, STAT2, TIFA, CD180, UNC93B1*) (Fig. S5E). Similarly, transcripts associated with antiviral responses (*ISG15, TRIM25, DHX58, USP18, DDX60*) (Fig. S5D) were particularly highly expressed in G2 at baseline and downregulated with spermidine.

Taken together, the scRNA-seq analysis points towards pro-proliferative and anti-senescent effects of spermidine in B cells. Other DEG signatures include ER stress, metabolism and inflammation, which are all tightly linked to autophagy and known to play a key role in B cells that differentiate into plasma cells[42,43]. This may explain the increase in anti-spike IgG secretion and improved vaccine response after spermidine.

We previously demonstrated that spermidine induces autophagy via TFEB. Building on this, we examined TFEB targets across lymphocyte subsets. Interestingly, most TFEB-regulated genes were significantly upregulated in B cells (Fig. 3L-M and S5G), particularly in seronegative vaccinees (G2) memory B cells (Fig. 3M), while CD8 and CD4 T cells exhibited smaller transcriptional increases upon spermidine treatment (Fig. S5H,I). This DEG pattern suggests that spermidine specifically induces autophagy and the TFEB pathway in B cells at this timepoint. Interestingly, among the upregulated genes is *MCOLN1*,

which activates calcineurin. Calcineurin dephosphorylates TFEB, leading to its nuclear translocation[44]. Notably, we did not find any other altered biological process signature in T cells.

Spermidine supplementation enhances autophagy and eIF5A hypusination.

To validate the data observed by scRNA-seq and understand the mechanism by which spermidine improves the adaptive immune response to SARS-CoV-2 vaccination, we first used flow cytometry-based staining for lipidated LC3 as described previously[29]. Two weeks after spermidine treatment, both B cells and $CD8^+$ T cells, but not $CD4^+$ T cells (Fig. 4A-C, respectively), showed significantly increased autophagic flux. Notably, this is the first report confirming the autophagy-inducing properties of spermidine supplementation *in vivo* in humans.

Spermidine is a critical substrate in the hypusination reaction of eIF5A, which is required for its activity as a translation elongation factor, specifically for hard-to-translate amino acid motifs[45] (Fig. 4D). We measured spermidine content in whole PBMCs by mass spectrometry (Fig. 4E) and eIF5A hypusination (Fig. 4F) by Western blot. Interestingly, only G2 showed a trend towards dynamic spermidine and hypusination levels, suggesting an increase at weeks 2 and 13 and subsequent decrease at week 37 after the washout period (Fig. 4E,F).

Due to the expected high variability in whole-PBMC analyses and the small cohort size, we correlated individual spermidine levels and hypusinated eIF5A across the groups with anti-spike IgG levels. Whereas we found little correlation in placebo and G1, there was a distinct and significant correlation in G2 between intracellular spermidine levels and hypusinated eIF5A at weeks 2 and 13 (Fig. 4G-I). These data suggest that spermidine increases autophagic flux in lymphocytes, probably via the hypusination of eIF5A, which likely accounts for improved vaccination responses. Amongst other proteins, hypusinated eIF5A facilitates the translation of *TFEB*, a major transcriptional regulator of autophagy and lysosome protein expression (Fig. S6A). TFEB protein expression, measured by flow cytometry, increased exclusively in CD4 T (Fig. S6B), but not in CD8 T (Fig. S6C) or B cells (Fig. S6D), following spermidine supplementation.

Moreover, we observed a negative correlation in G2 PBMCs between senescence markers and spermidine or hypusinated eIF5A (Fig. 5A), indicating that as spermidine and hypusinated eIF5A levels rise, senescence markers decrease. These findings suggest that spermidine improves vaccine responses by promoting eIF5A hypusination and reducing immune cell senescence. Furthermore, senescence markers could help identify older adults who do not respond well to vaccines.

Discussion

Many individuals, particularly older adults, exhibit insufficient immune responses to vaccination due to a combination of factors, including age, genetic predisposition, health status, and environmental stressors, with immunosenescence being a principal contributing factor. This decline in immune function, driven in part by reduced autophagy in immune cells, contributes to both vaccine failure and broader age-related

health conditions. We conducted an experimental clinical study to determine whether spermidine enhances autophagy and can affect vaccine responses in older humans, building on our previous findings that it restores B and T cell function through autophagy *in vitro* and in preclinical mouse models[29,38]. Antibody responses, crucial for vaccine efficacy[46], depend on functional B cell subsets, which decline with age[47]. Our data show that spermidine treatment induced autophagy in B cells, without altering B cell subset proportions, leading to significantly increased IgG secretion, spike-specific memory B cells, and enhanced neutralizing activity against SARS-CoV-2 strains, particularly in those with initially weak responses. This is the first evidence of spermidine, or any polyamine, inducing such effects in humans.

Spermidine acts primarily via the hypusination of eIF5A, which leads to enhanced *TFEB* translation and autophagy[38]. Our data show that following spermidine treatment, TFEB increased exclusively in CD4 cells, but not CD8 T or B cells, while autophagy was increased in B cells and CD8 T cells. This discrepancy may stem from different reasons: as the kinetics of *TFEB* translation and autophagy induction in different cell subsets have not been studied, we may have missed the time window for the spermidine-eIF5A-TFEB axis in some cell types. However, TFEB targets and genes mapped to the autophagy pathway were highly enriched across different cell types, with a particularly striking enrichment in B cells upon spermidine treatment. This enrichment was associated with an improved vaccine response, highlighting the pivotal role of spermidine and autophagy in enhancing immune responses in B cells. Notably, TFEB is more highly expressed in B than T cells and has higher expression profiles in memory versus naïve cells[48]. In this context, the limited dose of 6 mg spermidine used in our study could be primarily used by B cells to sustain the high synthetic demands of eIF5A hypusination. Future clinical trials should thus investigate whether higher doses elicit effects in T cells.

We cannot exclude that spermidine also acts on other cells that we could not characterise such as Tfh in the germinal center, antigen presenting cells and others in the immune microenvironment. Overall, these results indicate that spermidine's ability to induce autophagy and activate the TFEB pathway is a key factor in its selective enhancement of B cell function, providing insights into the molecular mechanisms underlying the observed improvements in B cell responses.

Spermidine's effects were observed in a subset of 8 out of 20 participants with low vaccine-specific IgG levels at baseline. To explore the differences between seropositive and seronegative individuals at baseline, we performed scRNA-seq on 5 donors from each group. After two weeks of spermidine treatment, B cells in responders showed increased expression of genes related to B cell signaling, ER stress, cell cycle regulation, DNA repair, and autophagy.

A key difference may be the elevated senescence markers in seronegatives, as immune cell senescence impacts vaccine efficacy, especially in the elderly[5,49–51]. Notably, two weeks of spermidine reduced senescence markers, including p16 (*CDKN2A*), which is linked to cellular aging. Spermidine likely promotes autophagic degradation of p16, as previous studies have shown its accumulation when autophagy is inhibited[52]. These findings suggest that spermidine mitigates replicative senescence in

aged B cells, potentially enhancing neutralizing antibody production and affinity maturation in germinal centers (GCs). Spermidine may either boost GC reactions by increasing proliferation or stimulate memory B cells to enhance antibody secretion.

Notably, at baseline these individuals also had a uniformly upregulated innate immune response (TLR signature and anti-viral immune response), which could indicate a subset resembling age-related B cells (ABC) which contribute to inflammaging via increased TLR signalling[53]. Interestingly, their abundance correlates with lower neutralising antibodies to the SARS-CoV-2 vaccine[54] placing them as a predictive biomarker for older individuals that would benefit from spermidine supplementation during vaccination.

Our study has limitations. First, the small sample size limits generalizability, and future studies should include larger cohorts and vaccines that are less effective in older adults, such as influenza. Second, our analysis was limited to naïve and memory B cells due to blood sampling constraints, while greater effects may be seen in long-lived plasma cells from bone marrow.

Despite these limitations, our study offers valuable insights into how spermidine rejuvenates cells through autophagy. It demonstrates that a daily dose of 6 mg is safe and supports the potential development of spermidine-based immune enhancers for older adults. Additionally, it underscores the utility of immune senescence markers as predictive biomarkers for vaccine responses in older individuals, which could help identify poor responders and address key challenges when vaccinating older adults.

Materials and Methods

Human participants and ethics statement

40 volunteers aged 65 or older participated in a double-blinded, randomized, controlled, experimental medicine study to determine the effects of daily spermidine supplementation with spermidine-rich wheat germ extract (spermidineLIFE®) on cellular immune responses to SARS-CoV-2 vaccination in older adults (ClinicalTrials.gov: NCT0542154). The spermidine-rich wheat germ extract (spermidineLIFE®) and placebo were provided by The Longevity Labs GmbH (TLL). The study was reviewed and approved by the University of Oxford, Medical Sciences Interdivisional Research Ethics Committee (MS IDREC), under ethical approval R75468/RE003. Inclusion criteria were age of 65 or more; capacity to provide written consent; and receipt of 3 doses of any licensed COVID vaccine at least 8 weeks before recruitment. Exclusion criteria were: acute illness; use of systemic steroids for more than one week, chronic (≥ 14 days in total) administration of immunosuppressants or other immune-modifying drugs in the 3 months prior to first study intervention; receipt of blood, blood products and/or plasma derivatives or any immunoglobulin preparation in the 3 months prior to first study intervention; immunosuppressive medical conditions or diabetes; allergy to spermidine supplements, their constituent parts, or gluten intolerance; spermidine supplementation at the point of recruitment or for 6 months prior.

Following informed consent, participants were assigned a unique study ID upon recruitment to the trial and randomised in a double-blinded in a 1:1 ratio to the placebo or spermidine arm. Participants attended 4 research appointments over a 37-week period at week 0, week 2, week 13 and week 37 (+/- 3 days) (Fig. S1).

The PI completed clinical case report forms to record details of participants' medical histories. This included: medical conditions; concurrent medication; allergies; COVID infection history and COVID vaccination history (vaccine type, date, number of doses); smoking, drug and alcohol use; age; and biological sex. Physical examination was performed at weeks 0 and 2, and abnormal findings were recorded. Anthropometric and vital signs were measured at all visits.

Venous blood (60 ml) was donated at weeks 0 and 2, whereas 50 ml was donated at weeks 13 and 37 with a qualified phlebotomist. BD vacutainers were used to collect venous blood samples for processing of PBMCs (EDTA), serology (SST) and spermidine (lithium heparin). Samples were processed for PBMC isolation within 3 hours of phlebotomy. 10 ml were analysed for urea and electrolytes, liver function tests, eGFR, random blood glucose, creatinine kinase, lipid profile, iron profile and full blood count at weeks 0 and 2, carried out by an accredited UK laboratory. 50 ml were analysed for immune cell activity and immune biomarkers at every timepoint.

Participants were dispensed 13 weeks of spermidine-rich wheat germ extract (spermidineLIFE®) or 13 weeks of placebo supplements (rice flour). Participants taking spermidine-rich wheat germ extract ingested 6 mg of powdered spermidine a day for 13 weeks. Participants in the placebo arm ingested the same weight of rice flour. Participants were asked to report any adverse events or reactions to the PI. Compliance with the supplement/placebo, and adverse reactions/events were monitored at the week 2, week and week 13 visits and recorded in a case report form.

Unscheduled visits (remote and in person) were arranged if a participant developed symptoms of COVID or had a positive swab. COVID infection and booster vaccine doses (timing and type of vaccine) were reported at each timepoint for the duration of the trial. Adverse events and reactions were reported to the Sponsor and investigated by the PI at an unscheduled visit as required (Fig. 1). Participants’ mean age was 72.5 years (median: 71, range: 65–81). 18 participants were male and 22 were female. All participants were White British. One participant withdrew due to travel difficulties and a further participant was recruited. Study visits were conducted ± 3 days from intended timepoints. At the time of recruitment, week 0 and week 2, all participants reported no previous history of confirmed COVID-19 or a positive swab or antibody test for COVID-19. Recruitment to the study began in September 2021 as the third SARS-CoV-2 vaccine booster was rolled out across the UK.

PBMCs and serum preparation

Serum was separated from whole blood from each time point using a 5 ml SSTII BD vacutainer (Becton Dickinson) as per manufacturer’s instructions, then stored at -70 ℃ in 0.5 ml aliquots until analyzed.

PBMCs were separated from red blood cells and plasma by overlaying 30 ml of EDTA-anticoagulated blood (pooled from K2E BD vacutainers) over 15 ml Histopaque-1077 Hybri-Max medium in a sterile 50 ml Falcon tube using aseptic methods, then separated by centrifugation at 500 xg, 25**°**C for 30 min. Following separation 4 x 1 ml aliquots of plasma were archived at -70**°** C for later, prior to removing the PBMC layer and washing by centrifugation (800 xg) in sterile, serum-free RPMI-1640 culture medium (Sigma-Aldrich). Cells were counted using an automated Cellometer Vision (Nexcelom Bioscience) quantifying live and dead cells using AO/PI Viastain. PBMCs were then resuspended in sterile foetal calf serum containing 10% DMSO to a final concentration of $10^{\wedge 6}$cells/ml (1 ml aliquots in cryovials) prior to storing in liquid nitrogen until required. One 6 ml lithium BD vacutainer was collected at each timepoint for spermidine quantification and was separated as above for EDTA samples except that 0.75 ml plasma was aliquoted, and separation utilized 3 ml Histopaque in a sterile 15 ml falcon tube.

Anti-spike IgG ELISA

Serum samples were used to measure and quantitate the immunoglobulin G (IgG) antibodies against human SARS-CoV-2 spike. Briefly SARS-CoV-2 Spike (Trimer) IgG protein (Native Antigen) was used to coat ELISA plates with 50 µl/well at a concentration of 1 ug/ml overnight. Serum samples were diluted in casein and plated in 96-well plates in triplicate and left for 2 h in a 20˚C incubator. Standard curve was made from a reference pool (1:2 serial dilution) with positive controls. Plates were washed 6 times with DPBS-T (0.05%). Anti-human IgG (γ-chain specific) alkaline phosphatase secondary antibody was added at 1:1000 and incubated for 1 hour. Plates were washed 6 times with DPBS-T (0.05%). 100 µl of pNPP substrate development buffer was added. Plates were read at OD405 nm on the BioTek ELx800 Microplate Reader with Gen5 ELISA software (v3.04).

T Cell Interferon-gamma (IFN-γ) ELISpot Assay

T cell interferon-gamma (IFN-γ) ELISpot Assay was performed following the Standard Operating Procedure as published previously[55]. After thawing of cryopreserved PBMCs, cells were rested for 3–6 h at 37°C, 5% CO2 in R10 media: RPMI 1640 (Sigma Aldrich, R0883) supplemented with 10% (v/v) Foetal Bovine Serum (FBS, Sigma Aldrich, F7524), 2mM L-Glutamine (Sigma Aldrich, G7513) and 1mM Penicillin/Streptomycin (Sigma Aldrich, P0781). PBMCs were then plated in duplicate at 200,000 cells/well in a MultiScreen-IP filter plate (Millipore, MAIPS4510) previously coated with capture antibody (clone 1-D1K, Mabtech, 3420-3-1000) and blocked with R10. PBMCs were stimulated with overlapping SARS-CoV-2 peptide pools (18-mers with 10 amino acid overlap, Mimotopes), representing the S1, S2 subunits, membrane (M) and nucleocapsid (N) at a final concentration of 2 ug/ml for 16–18 h in a humidified incubator at 37°C, 5% CO2. CEFT peptide pools (Proimmune, PX-CEFT) at a final concentration of 2 ug/ml and concanavalin A (ConA, Sigma, 11028-71-0) at a final concentration of 5 ug/ml were used as positive controls. DMSO (Sigma Aldrich, 67-68-5) in R10 was used as the negative control at an equivalent concentration to the DMSO content of the peptide pools. After incubation, cells were removed, and the wells were washed with PBS/0.05% (v/v) Tween20 (Sigma Aldrich, P3563-

5x10PAK). Secreted IFN-γ was detected by adding 1 µg/ml anti-IFN-γ biotinylated mAb (7-B6-1-biotin, Mabtech, 3420-6-1000) for 2–3 h, followed by 1 µg/ml streptavidin alkaline phosphatase (Vector Labs, SP-3020) for 1–2 h. Colour development was carried out using the 1-step™ NBT/BCIP substrate solution (Thermo Scientific, 34042) for 5 minutes at RT. The reaction was stopped by washing the wells with tap water. Air-dried plates were scanned and analysed with the ImmunoSpot® S6 Alfa Analyser (Cellular Technology Limited LLC, Germany). Antigen-specific responses were quantified by subtracting the mean spots of the negative control wells from the test wells, and the results were expressed as IFN-γ spot-forming units (SFU)/million PBMCs. Samples with a high background, defined as a mean spot value greater than 50 in the negative control were excluded from the analysis. A positive result was defined as greater than 35 SFU/million PBMC, which was calculated by the mean + 2 standard deviations (SD) of the negative control wells included in the analysis across the study.

Memory B cell FluoroSpot Assay

After thawing, PBMCs were cultured in 96-well round bottom plates (2 x 10^5 cells/well) for 72 h at 37°C, 5% CO2, with polyclonal stimulation containing 1 µg/ml R848 and 10 ng/ml IL-2 from the StimPacl: Memory B cells, Human (Mabtech, 3660-1). Stimulated PBMCs were then added at 2 x 10^5 cells/well to FluoroSpot plates (Human IgA/IgG FluoroSpotFLEX kit, Mabtech, X-06G05R-1) coated with 10 µg/ml SARS-CoV-2 spike glycoprotein (The Native Antigen Company, REC31966) and nucleocapsid protein (The Native Antigen Company, REC31851) diluted in PBS (Gibco, 10010-023), and 1X PBS (negative control wells). In addition, 6.6 x 10^3 cells/well were added to positive control wells coated with total anti-immunoglobin at a concentration of 15 µg/ml (Mabtech, FSX-05R-1). Plates were incubated for 18 h in a humidified incubator at 37°C, 5% CO2, and developed according to the manufacturer's instructions (Mabtech, X-06G05R-1). Analysis was carried out with AID ELISpot software 8.0 (Autoimmun Diagnostika). All samples were tested in duplicate, and memory B cell IgG response was measured as antibody spot-forming units (SFU) per million PBMCs with the mean spots of the negative control wells (PBS) subtracted.

Neutralisation antibodies (ACE2 inhibition assay)

The percentage of ACE2 inhibition of antibodies against the SARS-CoV-2 spike antigens of Wuhan (WT) and other variants (B.1.1.7, B.1.351, B.1.526.1, B.1.617, B.1.617.1, B.1.617.2, B.1.617.3, P.1, and P.2) was determined using the V-PLEX SARS-CoV-2 Panel 13 (ACE2) Kit (Meso Scale Diagnostics, K15466U-2). The assay was performed according to the manufacturer's instructions, with all incubations at room temperature with shaking at 600 RPM. Briefly, the plates were blocked with Blocker A solution (150 µL/well) for 30 minutes. Wells were washed three times with 150 µL wash buffer (1x), followed by the addition of samples (25 µL/well, diluted 1:100 in Diluent 100) and the ACE2 Calibration Reagent (25 µL/well) for 1 h. The SULFO-TAG Human ACE2 Protein was then added to the plate (25 µL/well) for 1 h, after which the wells were washed once more. Finally, MSD GOLD Read Buffer B (150 µL/well) was added, and the plate read with the MESO® SECTOR S 600 instrument.

Surface staining for flow cytometry

PBMCs were plated in a 6-well plate with 4 ml of R10 and rested overnight. The cells were then washed with PBS containing 5% Fetal Calf Serum (FCS) and resuspended in FACS buffer (PBS; 2% FCS; 5 nM EDTA) comprising various surface marker antibodies (Supplementary Table 4) at 4°C for 20 min in the dark. Fc block was added to the antibody mix to minimise non-specific antibody staining. Upon staining, the cells were washed in FACS buffer and either proceeded for intracellular staining, or direct acquisition using Cytek Aurora® and SpectroFlo® software. Gating strategies to determine cellular composition of B cells and $CD4^+$ and $CD8^+$ T cells (Fig. S7A). Acquired data were analysed using FlowJo (v10.8.1).

Intracellular staining for flow cytometry

PBMCs were stimulated in R10 using 1µL of Cell Activation Cocktail with Brefeldin A (Biolegend, Cat N 423304) for 3 h at 37°C. Unstimulated cells were also used as a control. Upon surface marker staining, cells were fixed using 100 µL Fixation buffer (BD, 51-2090KZ) for 20 minutes at room temperature in the dark. Following fixation, the cells were washed and permeabilised with 100 µL permeabilization buffer (BD, 51-2091KZ) for 15 minutes in the dark and washed again before the intracellular staining. A cocktail of intracellular markers, including TFEB (Fig. S7B-C) and senescence markers (Fig S8A-D), was used for staining, as indicated in Supplementary Table 4, and the cells were incubated in the dark for 30 minutes at room temperature. The cells were then washed twice with permeabilization buffer and resuspended in FACS buffer before data acquisition.

Autophagic flux assay for flow cytometry

Autophagy levels in PBMCs were assessed using the FlowCellect Autophagy LC3 antibody-based assay kit (FCCH100171) and measured after 2 h of treatment with bafilomycin A1 (10 nM BafA1, Cayman Chemical, cat N 11038) or vehicle (DMSO only) (Fig. S6B). In brief, cells were stained with surface markers, as indicated above, and washed using Assay buffer in a 96-well U-bottom plate. Cells were treated with 0.05% saponin, centrifuged, and then with 1:20 FITC-conjugated anti-LC3 antibody in Assay buffer at 4°C for 30 minutes. The cells were then washed with Assay buffer and fixed with 2% PFA before acquisition using Cytek Aurora® and SpectroFlo® software. Autophagic flux was analysed using the LC3-II mean fluorescence intensity of (BafA1-Vehicle)/Vehicle.

Detection of polyamines from serum and human PBMCs

Polyamine extraction and quantification using high performance liquid chromatography coupled to mass spectrometry (LC-MS/MS) was performed according to[56] with modifications described in[57]. Briefly, 100 µl serum were mixed with stable isotope-labelled standards and subjected to TCA-based protein precipitation as described[56]. For cellular polyamines, one PBMC aliquot was thawn on ice, transferred into a 2 ml protein LoBind reaction tube (Eppendorf) and centrifuged at 1000 rcf, 4°C for 5 min. After centrifugation, the supernatant was removed completely, followed by addition of 125 µl stable-isotope labelled standard mix containing 400 ng/ml of each polyamine as reported previously[56]. Cells were then resuspended by vortexing and polyamines extracted through addition of 375 µl 6.25% trichloroacetic acid (TCA) and incubation for one hour on ice (with vortexing every 15 min).

After TCA extraction, both serum and PBMC samples were centrifuged at 25,000 rcf, 4°C for 10 min, and 150 µl aliquots of the supernatants were transferred to fresh 1.5-ml LoBind reaction tubes. PBMC cell extracts were processed in duplicates, while the remaining supernatant and cell pellet was stored at -80°C for later immunoblotting. Polyamine-containing supernatants were then derivatised after addition of 37.5 µl ammonium formate (2 M aqueous solution), 800 µl of ultra-pure water and 125 µl of 1 M Na_2CO_3 (aqueous solution adjusted at pH 10 using hydrochloric acid) using 20 µl isobutyl chloroformate (SIGMA) followed by a 15-min incubation at 35°C. After centrifugation for 1 min at 15,000 rcf, 800 µl supernatant was transferred to LoBind 96-deep-well plates (VWR International, 737–2544) and stored at − 80°C until further processing.

Preceding LC-MS/MS analysis, polyamine derivatives were extracted by SPE (Strata-X, Polymeric Reversed Phase, 96-well plate). SPE was conditioned with 500 ml acetonitrile, equilibrated with 500 ml distilled water containing 0.2% acetic acid. Trichloroacetic acid extracts were loaded onto the SPE and after two washing steps with 500 ml 0.2% acetic acid samples were eluted with 250 ml 80% acetonitrile containing 0.2% acetic acid. Eluted SPE extracts were subjected to LC-MS/MS (mobile phase: isocratic 80% acetontrile containing 0.2% acetic acid; flow rate 250 ml/min; HPLC column: Kinetex 2.6 mm C18 100A 50 mm 3 2.1 mm and TSQ Quantum Access Max coupled to an Ultimate 3000). MS conditions were set as previously published[57]. LC–MS/MS data were acquired and processed using Xcalibur v.4.0 Software (Thermo Fisher Scientific). Finally, serum spermidine concentrations were normalized to each patient's baseline value. For PBMC polyamines, duplicate spermidine values were averaged (values with > 30% difference between technical replicates (12/154 samples) were excluded), followed by normalization to each patient's baseline value.

PBMC immunoblotting

The pellet after the TCA-based polyamine extraction was further processed for immunoblotting. After thawing on ice, the remaining polyamine-containing supernatant was completely removed following centrifugation for 5 min at 10,000 rcf, 4°C. The pellet was then resuspended on ice in 90 µl final sample buffer (62.5 mM Tris/HCl, pH 6.8, 2% sodium dodecylsulfate [SDS], 8.7% glycerol, 0.004% bromophenol blue, 120 mM dithiothreitol) and 10 µl untitrated 1 M Tris solution were added to adjust the pH. The resuspended pellet was vortexed for 10 min at 4°C. After a brief spin in a cooled tabletop centrifuge, the samples were heated for 5 min at 95°C and stored at -20°C upon immunoblotting.

Aliquots used for immunoblotting were thawed on ice and re-heated just before use. For protein separation, 5 µl were loaded on 4–12% NuPAGE Bis-Tris gels (ThermoFisher Scientific). Electrophoresis was performed at room temperature at 100–140 V with 1x MOPS SDS running buffer (ThermoFisher Scientific #NP000102). Proteins were wet-transferred to methanol-activated 0.45 µm PVDF membranes (Roth # T830.1) at 220 mA for 90 min using transfer buffer (10 mM CAPS/NaOH pH 11, 10% methanol). After blotting, membranes were blocked with blocking solution (1% dry milk powder in Tris-buffered saline [TBS] + 0.1% Tween-20 [TST], pH 7.4) for 1 hour and then incubated with the primary antibodies overnight at 4°C. After three washing steps in TST for 5 minutes, membranes were incubated with

secondary, horse radish peroxidase (HRP)-linked antibodies for 1 hour at room temperature. After three washing steps in TST for 5 minutes, signals were detected with a ChemiDoc detection system (Bio-Rad) and Clarity Western ECL Substrate (Bio-Rad) using the 'optimal exposure' setting. For re-probing membranes, Restore PLUS Western Blot Stripping Buffer (ThermoFisher Scientific #46430) was used according to the manufacturer's protocol. Band intensities were quantified using ImageLab 5.2 (Bio-Rad) using the rectangular volume tool with local background adjustment. Primary antibodies were anti-hypusine (Merck #ABS1064-I, 1:1000), anti-eIF5A (BD #611977), anti-GAPDH clone GA1R (ThermoFisher Scientific #MA5-15738, 1:10,000). Secondary antibodies were HRP-linked anti-mouse IgG (Sigma #A9044, 1:10,000) or HRP-linked anti-rabbit IgG (Sigma #A0545, 1:10,000). All antibodies were diluted in TST with 1% dry milk powder.

Single-cell RNA sequencing

Sample Collection and Pooling

Fifteen patient samples (5 per group) for two time points (week 0 and week 2) were collected and divided into two pools for analysis, using 10x Genomics (kit 1000414). The single-cell RNA sequencing (scRNA-seq) data from these pools were processed and analyzed using the Seurat[41] and clusterProfiler[58] packages in R.

Data Preprocessing and Integration

The scRNA-seq data from the two pools were initially loaded into R. The datasets from each pool were imported individually. These were then combined into a single Seurat object.

Within the combined object, the RNA assay was processed by joining the layers. The combined dataset was then normalized, and variable features were identified.

Subsequently, the data were scaled, and principal component analysis (PCA) was performed using RunPCA. To correct for batch effects and integrate the datasets, the Harmony integration method was applied to the PCA results through the IntegrateLayers function. Finally, Uniform Manifold Approximation and Projection (UMAP) was run on the integrated data based on the Harmony reduction.

Reference Mapping and Differential Expression Analysis

Seurat v4 Reference Mapping was utilized to annotate the peripheral blood mononuclear cell (PBMC) dataset[41,59]. For differential expression analysis, differentially expressed genes (DEGs) were identified for each cluster. The Seurat object was subsetted for each specific cluster, and the FindMarkers function was used to perform differential expression analysis, comparing conditions at 2 weeks to their respective baselines. DEGs were considered significant if they had an adjusted *p*-value (p_{adj}) < 0.1, using the Benjamini-Hochberg method.

Functional Enrichment Analysis

To understand the biological implications of the DEGs, functional enrichment analysis was performed using the clusterProfiler package (version 4.6.0)[58]. For each cluster, significant DEGs were extracted and subjected to Gene Ontology (GO) enrichment analysis using the enrichGO function. The analysis focused on biological processes (BP) with a q-value cutoff of 0.1, identifying key biological processes associated with the DEGs.

Statistical analysis

All graphs were plotted using GraphPad Prism software (v8.3.1). Data are presented as Tukey boxplots or violin plots with statistical comparisons using the Wilcoxon test. A threshold of significance of $p = 0.05$ was set, and p-values < 0.05, < 0.01 and < 0.001 were considered statistically significant.

Declarations

Competing interests

A.K.S. is a consultant for TLL The Longevity Labs GmbH and Oxford Healthspan, G.A. is a consultant for Oxford Healthspan. T.E. is a consultant for TLL The Longevity Labs GmbH. TLL has had no input into the trial design, results, analysis or manuscript.

Acknowledgements

We thank Dr Thomas Conrad and Dr Francesca Solinas from the Max-Delbrück-Centrum für Molekulare Medizin (MDC, Germany), for their help with experimental transcriptomics experiment. Dr. Nicholas Peckham, Senior Medical Statistician at the Oxford Clinical Trials Research Unit (OCTRU), for his assistance with the statistical analysis. Dr Jonathan Webber for his help with the flow cytometry experimental design. M. Hausl from Joanneum Research HEALTH, Graz, Austria, and A. Müller and L. Opriessnig from the Institute of Molecular Biosciences, University of Graz, Austria, for help with the polyamines measurement experiments. The Longevity Labs GmbH for providing the spermidine-rich wheatgerm extract (spermidineLIFE®) and placebo. This work was supported by grants from the Wellcome Trust to A.K.S. (Investigator award 220784/Z/20/Z), UK SPINE and TLL The Longevity Labs GmbH, Versus Arthritis grant 22617 to G.A. and University of Graz and by the Austrian Science Fund (FWF) grants P33957 and TAI6021000 to T.E.

References

1. Franceschi, C. *et al.* Inflamm-aging. An evolutionary perspective on immunosenescence. *Ann N Y Acad Sci* **908**, 244-254, doi:10.1111/j.1749-6632.2000.tb06651.x (2000).
2. Teissier, T., Boulanger, E. & Cox, L. S. Interconnections between Inflammageing and Immunosenescence during Ageing. *Cells* **11**, doi:10.3390/cells11030359 (2022).

3. COVID-19 confirmed deaths in England (to 31 December 2022): report - GOV.UK (www.gov.uk) accessed 20th May 2024)
4. Goodwin, K., Viboud, C. & Simonsen, L. Antibody response to influenza vaccination in the elderly: a quantitative review. *Vaccine* **24**, 1159-1169, doi:10.1016/j.vaccine.2005.08.105 (2006).
5. Goronzy, J. J. & Weyand, C. M. Understanding immunosenescence to improve responses to vaccines. *Nat Immunol* **14**, 428-436, doi:10.1038/ni.2588 (2013).
6. Osterholm, M. T., Kelley, N. S., Sommer, A. & Belongia, E. A. Efficacy and effectiveness of influenza vaccines: a systematic review and meta-analysis. *Lancet Infect Dis* **12**, 36-44, doi:10.1016/S1473-3099(11)70295-X (2012).
7. Palacios-Pedrero, M. A. *et al.* Signs of immunosenescence correlate with poor outcome of mRNA COVID-19 vaccination in older adults. *Nat Aging* **2**, 896-905, doi:10.1038/s43587-022-00292-y (2022).
8. Van der Wielen, M., Van Damme, P., Chlibek, R., Smetana, J. & von Sonnenburg, F. Hepatitis A/B vaccination of adults over 40 years old: comparison of three vaccine regimens and effect of influencing factors. *Vaccine* **24**, 5509-5515, doi:10.1016/j.vaccine.2006.04.016 (2006).
9. D'Acremont, V., Herzog, C. & Genton, B. Immunogenicity and safety of a virosomal hepatitis A vaccine (Epaxal) in the elderly. *J Travel Med* **13**, 78-83, doi:10.1111/j.1708-8305.2006.00001.x (2006).
10. Yen, Y. H. *et al.* Study of hepatitis B (HB) vaccine non-responsiveness among health care workers from an endemic area (Taiwan). *Liver Int* **25**, 1162-1168, doi:10.1111/j.1478-3231.2005.01157.x (2005).
11. Pritz, T. *et al.* Plasma cell numbers decrease in bone marrow of old patients. *Eur J Immunol* **45**, 738-746, doi:10.1002/eji.201444878 (2015).
12. McElhaney, J. E., Upshaw, C. M., Hooton, J. W., Lechelt, K. E. & Meneilly, G. S. Responses to influenza vaccination in different T-cell subsets: a comparison of healthy young and older adults. *Vaccine* **16**, 1742-1747, doi:10.1016/s0264-410x(98)00133-9 (1998).
13. Bernstein, E. D., Gardner, E. M., Abrutyn, E., Gross, P. & Murasko, D. M. Cytokine production after influenza vaccination in a healthy elderly population. *Vaccine* **16**, 1722-1731, doi:10.1016/s0264-410x(98)00140-6 (1998).
14. Hainz, U. *et al.* Insufficient protection for healthy elderly adults by tetanus and TBE vaccines. *Vaccine* **23**, 3232-3235, doi:10.1016/j.vaccine.2005.01.085 (2005).
15. Ward, J. K., Alleaume, C., Peretti-Watel, P. & Group, C. The French public's attitudes to a future COVID-19 vaccine: The politicization of a public health issue. *Soc Sci Med* **265**, 113414, doi:10.1016/j.socscimed.2020.113414 (2020).
16. Collier, D. A. *et al.* Age-related immune response heterogeneity to SARS-CoV-2 vaccine BNT162b2. *Nature* **596**, 417-422, doi:10.1038/s41586-021-03739-1 (2021).
17. McElhaney, J. E. *et al.* The effect of influenza vaccination on IL2 production in healthy elderly: implications for current vaccination practices. *J Gerontol* **47**, M3-8, doi:10.1093/geronj/47.1.m3

(1992).

18. Weinberger, B. Vaccines for the elderly: current use and future challenges. *Immun Ageing* **15**, 3, doi:10.1186/s12979-017-0107-2 (2018).
19. Fulop, T. *et al.* Immunosenescence and Altered Vaccine Efficiency in Older Subjects: A Myth Difficult to Change. *Vaccines (Basel)* **10**, doi:10.3390/vaccines10040607 (2022).
20. van der Klaauw, A. A. *et al.* Accelerated waning of the humoral response to COVID-19 vaccines in obesity. *Nat Med* **29**, 1146-1154, doi:10.1038/s41591-023-02343-2 (2023).
21. Klaus, E. Vaccine non-responders and severe adverse events. *Open Access Government* doi:10.56367/OAG-042-11222 (2024).
22. Lopez-Otin, C., Blasco, M. A., Partridge, L., Serrano, M. & Kroemer, G. Hallmarks of aging: An expanding universe. *Cell* **186**, 243-278, doi:10.1016/j.cell.2022.11.001 (2023).
23. Clarke, A. J. & Simon, A. K. Autophagy in the renewal, differentiation and homeostasis of immune cells. *Nat Rev Immunol* **19**, 170-183, doi:10.1038/s41577-018-0095-2 (2019).
24. Metur, S. P. & Klionsky, D. J. Adaptive immunity at the crossroads of autophagy and metabolism. *Cell Mol Immunol* **18**, 1096-1105, doi:10.1038/s41423-021-00662-3 (2021).
25. Schmauck-Medina, T. *et al.* New hallmarks of ageing: a 2022 Copenhagen ageing meeting summary. *Aging (Albany NY)* **14**, 6829-6839, doi:10.18632/aging.204248 (2022).
26. Cuervo, A. M. & Dice, J. F. Lysosomes, a meeting point of proteins, chaperones, and proteases. *J Mol Med (Berl)* **76**, 6-12, doi:10.1007/s001090050185 (1998).
27. Sarkis, G. J., Ashcom, J. D., Hawdon, J. M. & Jacobson, L. A. Decline in protease activities with age in the nematode Caenorhabditis elegans. *Mech Ageing Dev* **45**, 191-201, doi:10.1016/0047-6374(88)90001-2 (1988).
28. Hughes, A. L. & Gottschling, D. E. An early age increase in vacuolar pH limits mitochondrial function and lifespan in yeast. *Nature* **492**, 261-265, doi:10.1038/nature11654 (2012).
29. Alsaleh, G. *et al.* Autophagy in T cells from aged donors is maintained by spermidine and correlates with function and vaccine responses. *Elife* **9**, doi:10.7554/eLife.57950 (2020).
30. Pyo, J. O. *et al.* Overexpression of Atg5 in mice activates autophagy and extends lifespan. *Nat Commun* **4**, 2300, doi:10.1038/ncomms3300 (2013).
31. Simonsen, A. *et al.* Promoting basal levels of autophagy in the nervous system enhances longevity and oxidant resistance in adult Drosophila. *Autophagy* **4**, 176-184, doi:10.4161/auto.5269 (2008).
32. Ulgherait, M., Rana, A., Rera, M., Graniel, J. & Walker, D. W. AMPK modulates tissue and organismal aging in a non-cell-autonomous manner. *Cell Rep* **8**, 1767-1780, doi:10.1016/j.celrep.2014.08.006 (2014).
33. Mortensen, M. *et al.* The autophagy protein Atg7 is essential for hematopoietic stem cell maintenance. *J Exp Med* **208**, 455-467, doi:10.1084/jem.20101145 (2011).
34. Stranks, A. J. *et al.* Autophagy Controls Acquisition of Aging Features in Macrophages. *J Innate Immun* **7**, 375-391, doi:10.1159/000370112 (2015).

35. Xu, X. *et al.* Autophagy is essential for effector CD8(+) T cell survival and memory formation. *Nat Immunol* **15**, 1152-1161, doi:10.1038/ni.3025 (2014).
36. Puleston, D. J. *et al.* Autophagy is a critical regulator of memory CD8(+) T cell formation. *Elife* **3**, doi:10.7554/eLife.03706 (2014).
37. Phadwal, K. *et al.* A novel method for autophagy detection in primary cells: impaired levels of macroautophagy in immunosenescent T cells. *Autophagy* **8**, 677-689, doi:10.4161/auto.18935 (2012).
38. Zhang, H. *et al.* Polyamines Control eIF5A Hypusination, TFEB Translation, and Autophagy to Reverse B Cell Senescence. *Mol Cell* **76**, 110-125 e119, doi:10.1016/j.molcel.2019.08.005 (2019).
39. Puleston, D. J. *et al.* Polyamines and eIF5A Hypusination Modulate Mitochondrial Respiration and Macrophage Activation. *Cell Metab* **30**, 352-363 e358, doi:10.1016/j.cmet.2019.05.003 (2019).
40. Lubas, M. *et al.* eIF5A is required for autophagy by mediating ATG3 translation. *EMBO Rep* **19**, doi:10.15252/embr.201846072 (2018).
41. Hao, Y. *et al.* Dictionary learning for integrative, multimodal and scalable single-cell analysis. *Nat Biotechnol* **42**, 293-304, doi:10.1038/s41587-023-01767-y (2024).
42. Raza, I. G. A. & Clarke, A. J. B Cell Metabolism and Autophagy in Autoimmunity. *Front Immunol* **12**, 681105, doi:10.3389/fimmu.2021.681105 (2021).
43. Pengo, N. *et al.* Plasma cells require autophagy for sustainable immunoglobulin production. *Nat Immunol* **14**, 298-305, doi:10.1038/ni.2524 (2013).
44. Medina, D. L. *et al.* Lysosomal calcium signalling regulates autophagy through calcineurin and TFEB. *Nat Cell Biol* **17**, 288-299, doi:10.1038/ncb3114 (2015).
45. Gutierrez, E. *et al.* eIF5A promotes translation of polyproline motifs. *Mol Cell* **51**, 35-45, doi:10.1016/j.molcel.2013.04.021 (2013).
46. Pollard, A. J. & Bijker, E. M. Publisher Correction: A guide to vaccinology: from basic principles to new developments. *Nat Rev Immunol* **21**, 129, doi:10.1038/s41577-020-00497-5 (2021).
47. Frasca, D., Diaz, A., Romero, M. & Blomberg, B. B. The generation of memory B cells is maintained, but the antibody response is not, in the elderly after repeated influenza immunizations. *Vaccine* **34**, 2834-2840, doi:10.1016/j.vaccine.2016.04.023 (2016).
48. Fernandez, M. R. *et al.* Disrupting the MYC-TFEB Circuit Impairs Amino Acid Homeostasis and Provokes Metabolic Anergy. *Cancer Res* **82**, 1234-1250, doi:10.1158/0008-5472.CAN-21-1168 (2022).
49. Akbar, A. N. & Henson, S. M. Are senescence and exhaustion intertwined or unrelated processes that compromise immunity? *Nat Rev Immunol* **11**, 289-295, doi:10.1038/nri2959 (2011).
50. Muller, L. *et al.* Age-dependent Immune Response to the Biontech/Pfizer BNT162b2 Coronavirus Disease 2019 Vaccination. *Clin Infect Dis* **73**, 2065-2072, doi:10.1093/cid/ciab381 (2021).
51. Lord, J. M. *et al.* Accelarated immune ageing is associated with COVID-19 disease severity. *Immun Ageing* **21**, 6, doi:10.1186/s12979-023-00406-z (2024).

52. Coryell, P. R. *et al.* Autophagy regulates the localization and degradation of p16(INK4a). *Aging Cell* **19**, e13171, doi:10.1111/acel.13171 (2020).
53. de Mol, J., Kuiper, J., Tsiantoulas, D. & Foks, A. C. The Dynamics of B Cell Aging in Health and Disease. *Front Immunol* **12**, 733566, doi:10.3389/fimmu.2021.733566 (2021).
54. Yam-Puc, J. C. *et al.* Age-associated B cells predict impaired humoral immunity after COVID-19 vaccination in patients receiving immune checkpoint blockade. *Nat Commun* **14**, 3292, doi:10.1038/s41467-023-38810-0 (2023).
55. Angyal, A. *et al.* T-cell and antibody responses to first BNT162b2 vaccine dose in previously infected and SARS-CoV-2-naive UK health-care workers: a multicentre prospective cohort study. *Lancet Microbe* **3**, e21-e31, doi:10.1016/S2666-5247(21)00275-5 (2022).
56. Magnes, C. *et al.* Polyamines in biological samples: rapid and robust quantification by solid-phase extraction online-coupled to liquid chromatography-tandem mass spectrometry. *J Chromatogr A* **1331**, 44-51, doi:10.1016/j.chroma.2013.12.061 (2014).
57. Costa-Machado, L. F. *et al.* Peripheral modulation of antidepressant targets MAO-B and GABAAR by harmol induces mitohormesis and delays aging in preclinical models. *Nat Commun* **14**, 2779, doi:10.1038/s41467-023-38410-y (2023).
58. Wu, T. *et al.* clusterProfiler 4.0: A universal enrichment tool for interpreting omics data. *Innovation (Camb)* **2**, 100141, doi:10.1016/j.xinn.2021.100141 (2021).
59. Hao, Y. *et al.* Integrated analysis of multimodal single-cell data. *Cell* **184**, 3573-3587 e3529, doi:10.1016/j.cell.2021.04.048 (2021).

Tables

Tables 1 and 2 are available in the Supplementary Files section.

Figures

Figure 1

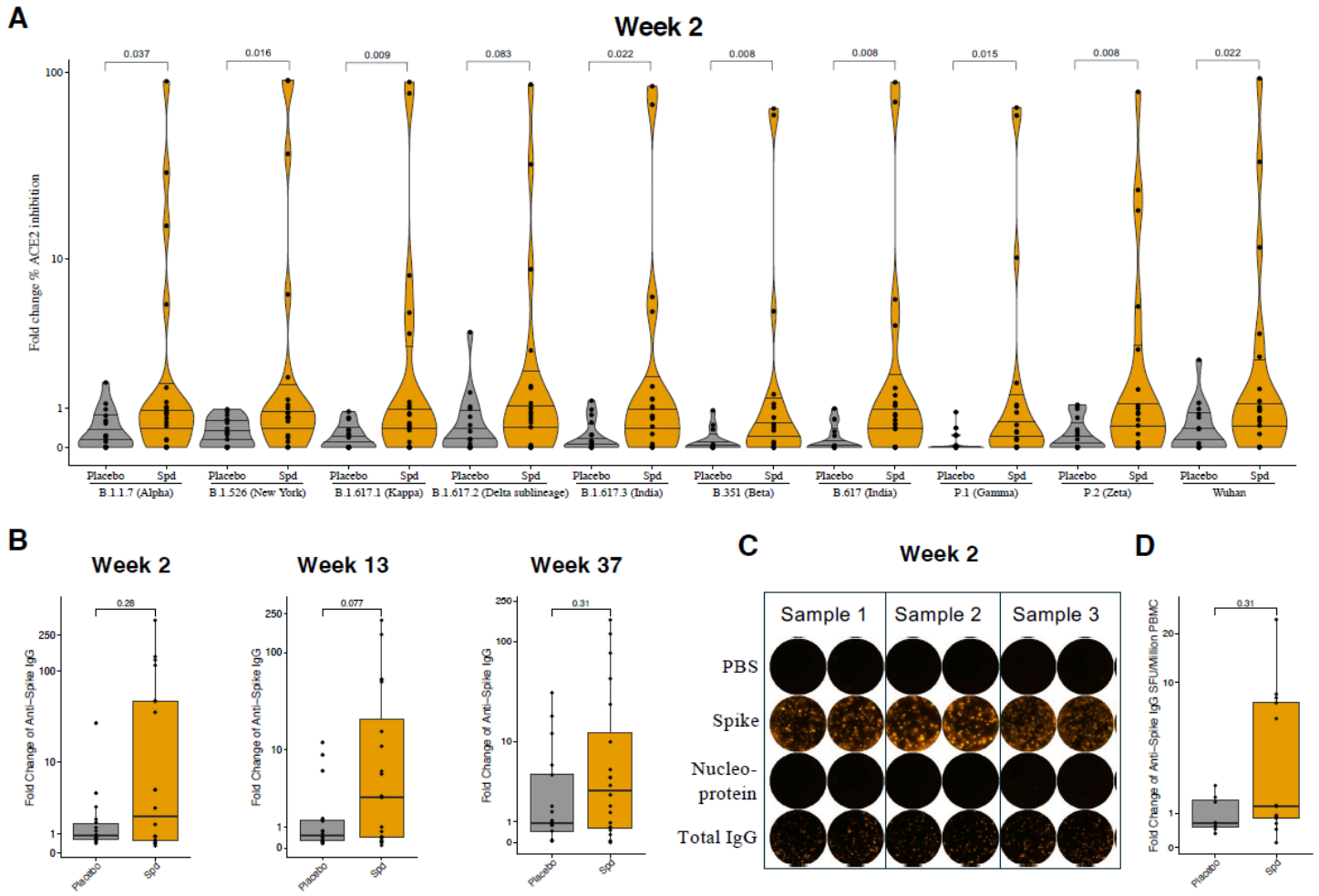

Figure 1

Enhanced vaccine responses observed with spermidine supplementation.

A: ACE2 inhibition (%) fold change from neutralisation antibody assay in placebo and spermidine groups at 2 weeks, against SARS-CoV-2 variants: Wuhan, P.2 (Zeta), B.1.1.7 (Alpha), B.1.617 (India), B.1.351 (Beta), B.1.526 (New York), B.1.617.2 (Delta), B 1.617.1 (Kappa), B.1.617.3 (India), P.1(Gamma). B: Anti-spike IgG fold change at (left panel) 2 weeks, (middle panel) 13 weeks, and (right panel) 37 weeks post spermidine (orange = Spd group, undivided). C: FluoroSpot example image for B cells in spike IgG plates. D: Anti-spike IgG fold change (from FluoroSpot) for PBMC-derived B cells 2 weeks post spermidine. Data are presented as violin plots or Tukey boxplots with statistical comparisons using the Wilcoxon test.

Figure 2

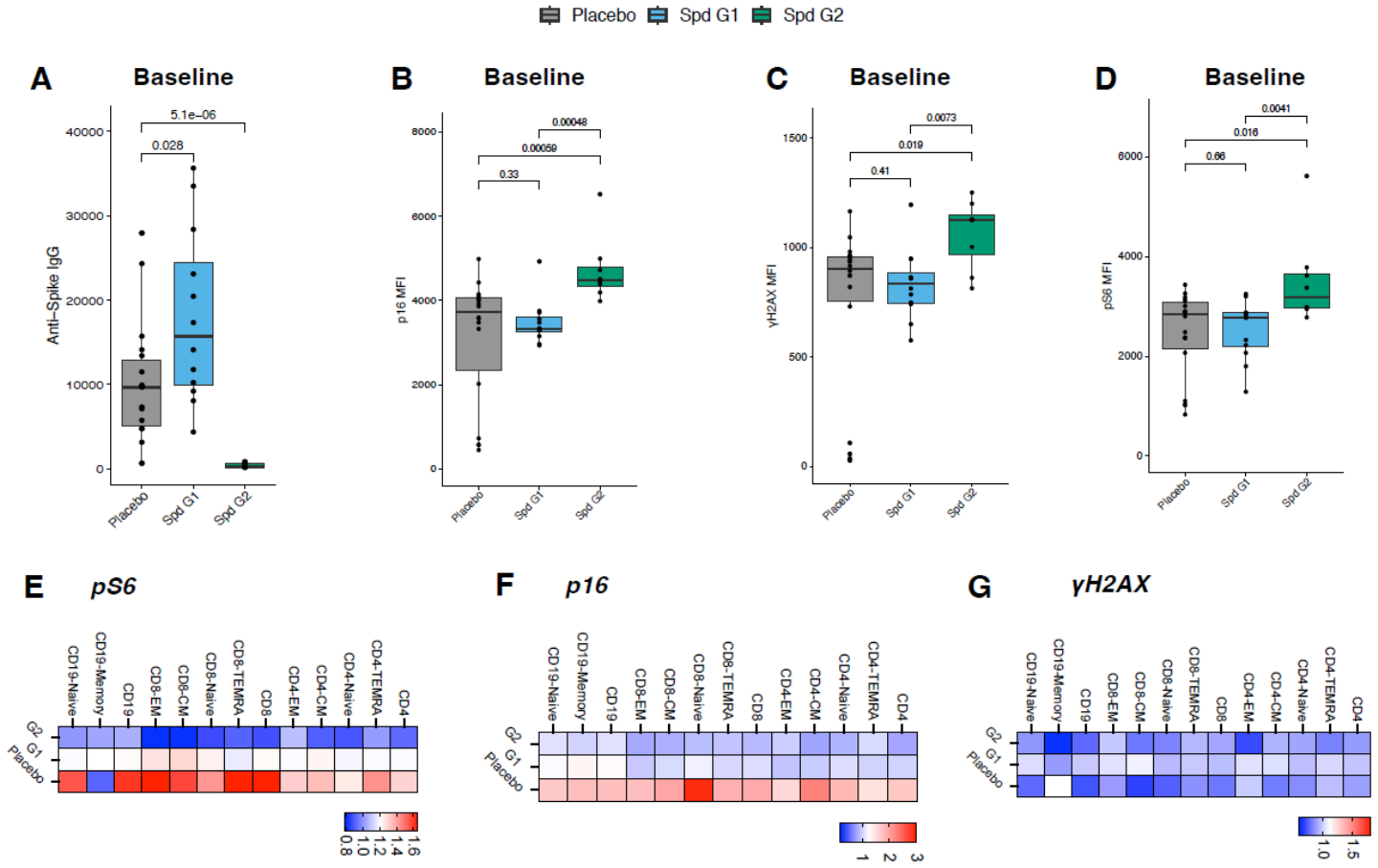

Figure 2

Spermidine treatment promotes senescent cell rejuvenation in vaccine non-responders, (Group 2, 'G2').

A: Anti-spike IgG intensity (ELISA) at baseline and 2 weeks post spermidine (Spd) for placebo (grey), Spd group 1 (G1, blue) and Spd group 2 (G2, green). **B-D:** PBMC baseline mean fluorescence intensity (MFI) of **(B)** p-16, (**C)** γ-H2AX, **(D)** pS6 in placebo and spermidine (Spd) groups 1 (G1) and 2 (G2). **E-G:** Senescence marker fold change heatmap between baseline and 2 weeks for **(E)** pS6, **(F)** p16, **(G)** γH2AX in CD4 T cell, CD8 T cell and B cell subsets. Data are presented as Tukey boxplots with statistical comparisons using the Wilcoxon test.

Figure 3

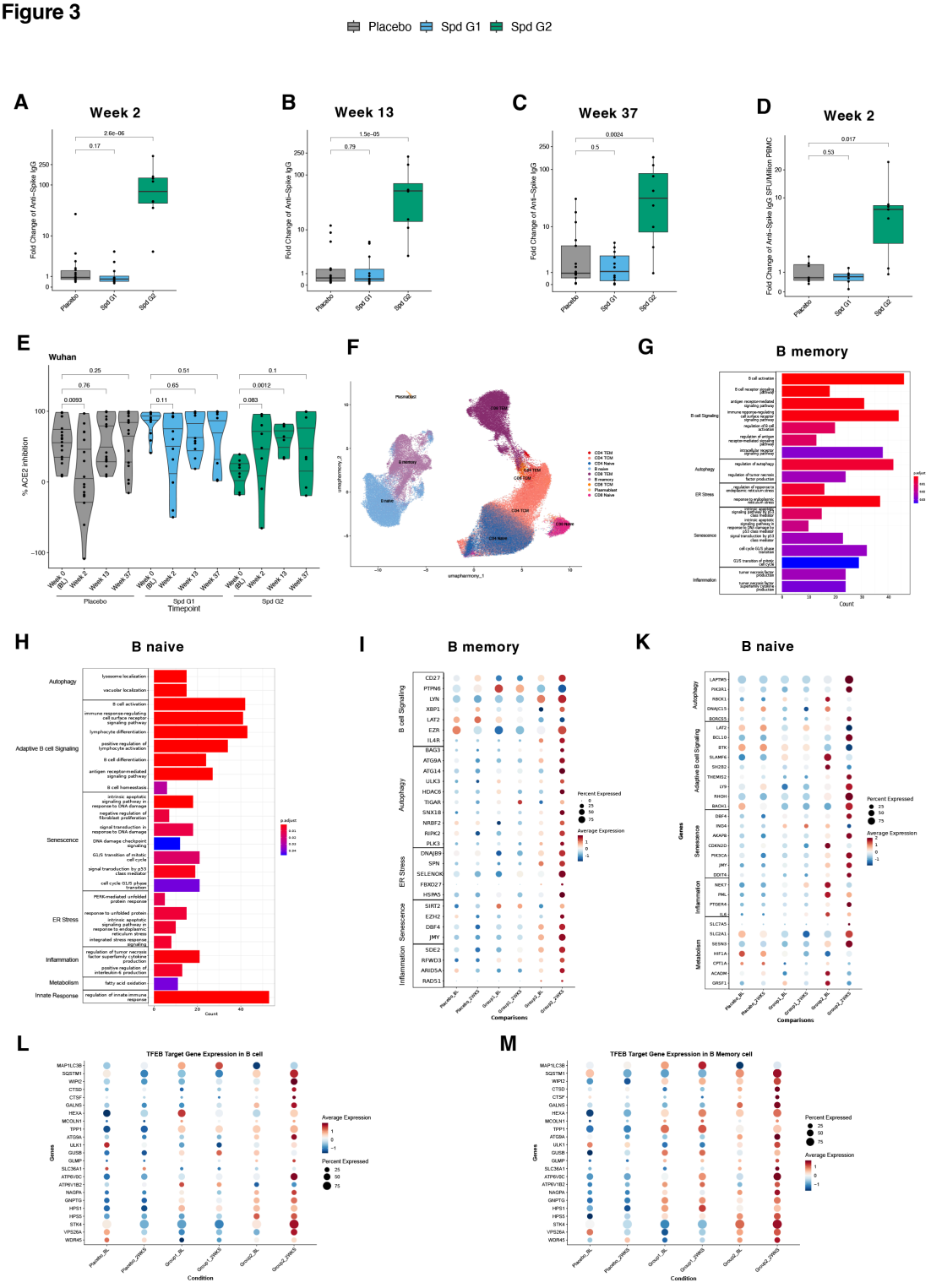

Figure 3

Spermidine treatment leads to significant modifications in B cell pathways and enhances their responses to the COVID-19 vaccine.

A-C: Anti-spike IgG fold change from baseline for placebo (grey), Spd group 1 (G1, blue) and Spd group 2 (G2, green) at (**A**) 2 weeks, (**B**) 13 weeks, and (**C**) 37 weeks post spermidine. **D:** Anti-spike IgG fold

change (from FluoroSpot) for PBMC-derived B cells 2 weeks post spermidine: placebo versus G1 and G2. **E:** ACE2 inhibition (%) across all groups and timepoints, from neutralisation antibody assay against SARS-CoV-2 Wuhan variant. Data are presented as Tukey boxplots or violin plots with statistical comparisons using the Wilcoxon test. **F-M:** scRNA-seq analysis of 5 volunteers in each group (spermidine G1 and G2, and placebo) at baseline (BL) and week 2. **F:** UMAP plot of PBMCs, with cell types (colors) identified by multimodal reference mapping using the Seurat annotated reference dataset. **G-H:** Pathway enrichment analysis of differentially expressed genes (DEGs) in (**G**) B memory cells and (**H**) naïve B cells, showing significantly enriched pathways. I-K: Gene expression (scaled) dot heatmaps and pathways of DEGs in (**I**) B memory cells, (**K**) naïve B cells. **L-M:**TFEB target gene expression (scaled) dot heatmaps and pathways of (**L**) B cells and (**M**) memory B cells.

Figure 4

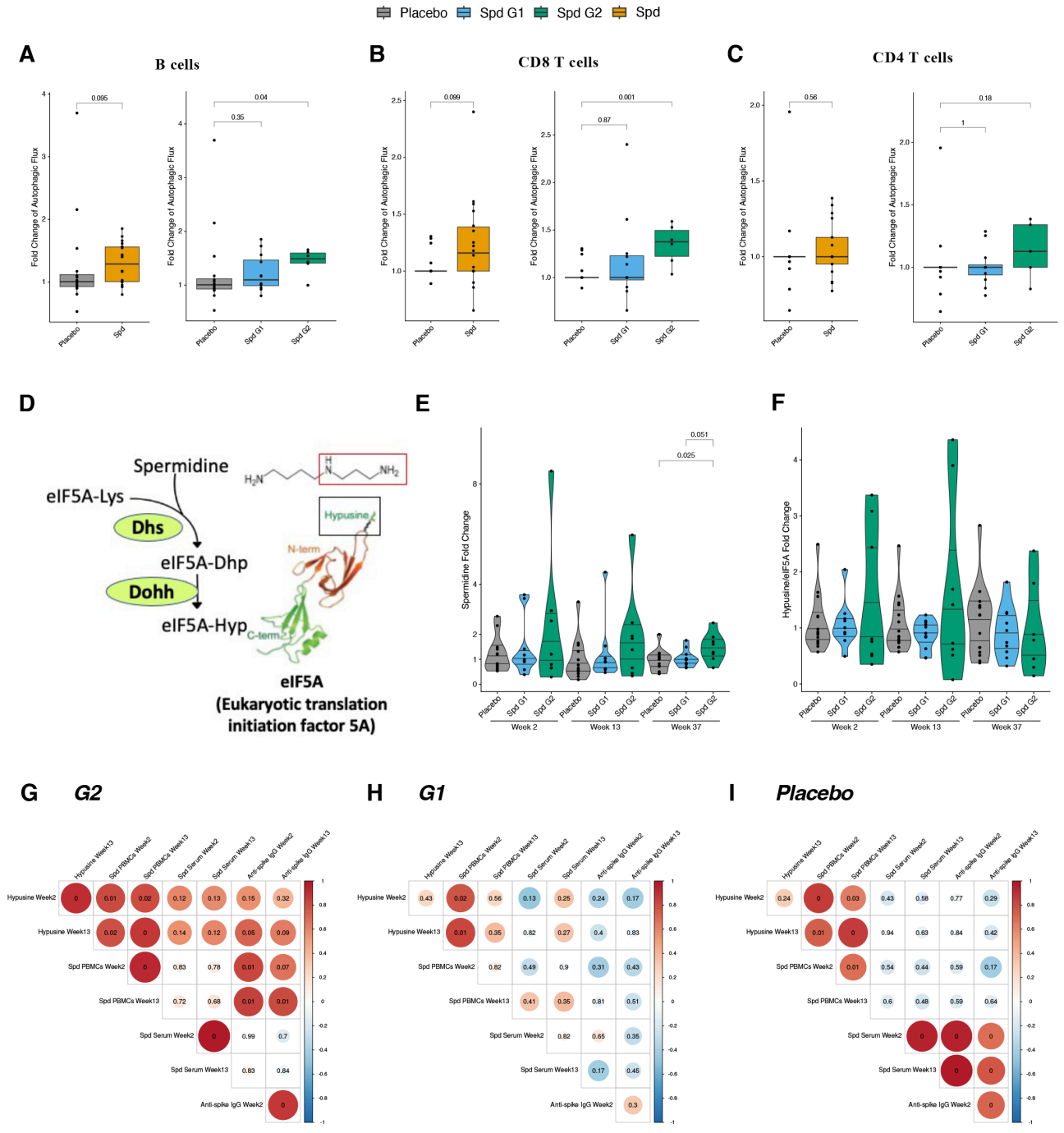

Figure 4

Spermidine supplementation triggers autophagy and correlates with anti-spike antibody levels.

Autophagic flux fold change 2 weeks post spermidine supplementation in **(A)** B cells, **(B)** CD8$^+$ T cells, (**C**) CD4$^+$ T cells. **D:** Schematic representation of the proposed mechanism of action of spermidine supplementation in eIF5A hypusination. **E:** Spermidine fold change in PBMCs (measured by LC-MS/MS).

F: Hypusinated eIF5A fold change in PBMCs, measured by Western blot. **G-I:** Example correlation matrices for G2 **(G)**, G1 **(H)**, and placebo **(I)**. Entries represent Pearson correlation coefficients between parameters: dot size denotes strength, colour denotes positive (red) or negative (blue), shade denotes higher (darker) or lower (lighter) absolute values, p-values are shown within dots. Annotations: spermidine (Spd); group 1 (G1); group 2 (G2). Statistical analyses in **A-F** were conducted using Wilcoxon tests and data are presented as Tukey boxplots or violin plots.

Figure 5

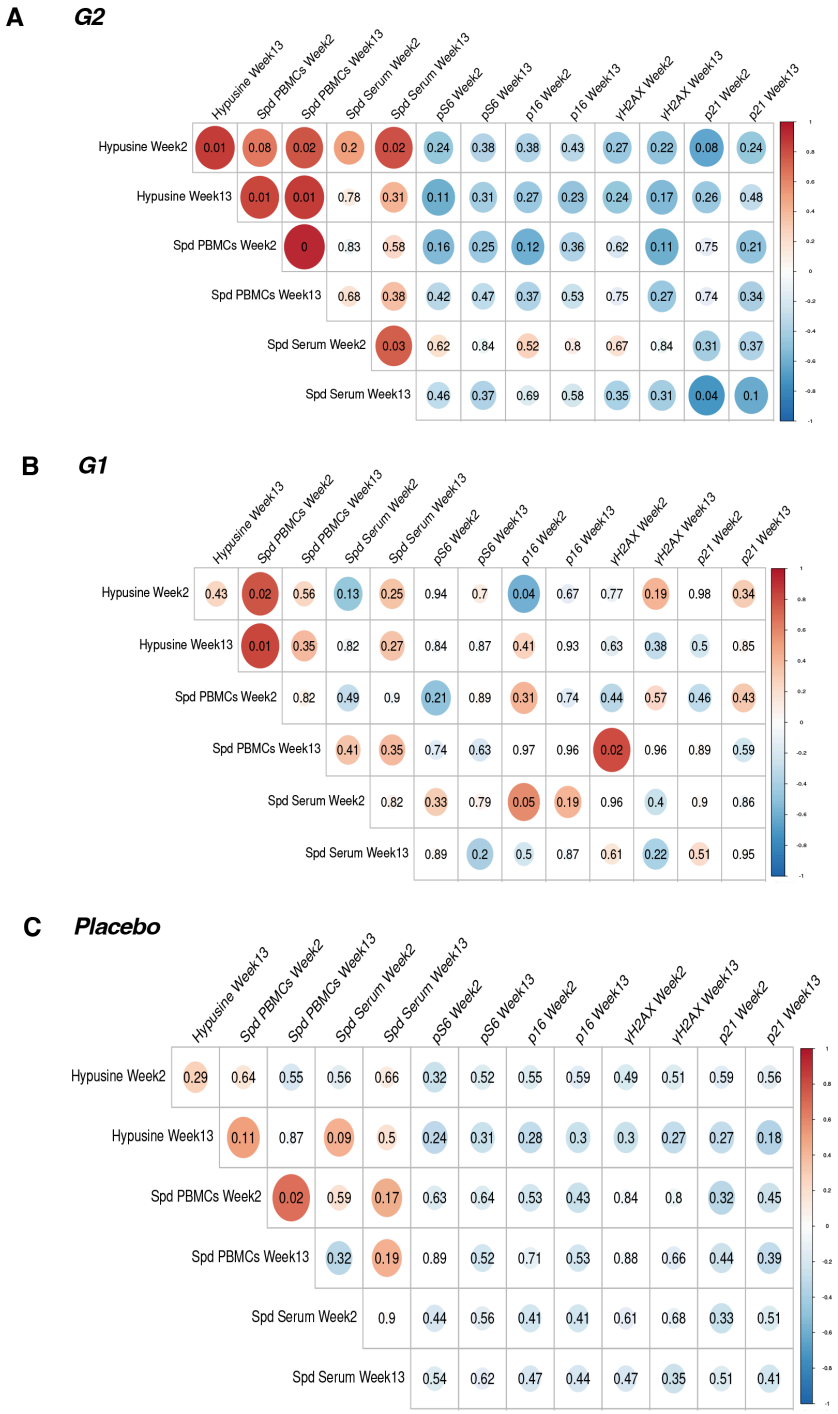

Figure 5

Correlations between senescence markers and spermidine levels across groups.

A-C: Example correlation matrices for **(A)** G2, **(B)** G1 and **(C)** placebo groups. Entries represent Pearson correlation coefficients between parameters: dot size denotes strength, colour denotes positive (red) or negative (blue), shade denotes higher (darker) or lower (lighter) absolute values, p-values are shown within dots. Statistical analyses were conducted using Wilcoxon tests.

Supplementary Files

This is a list of supplementary files associated with this preprint. Click to download.

- AlsalehetalTable1.docx
- AlsalehetalTable2.docx
- AlsalehetalSupplementarymaterialsclinicaltrailNatureaging20122024.docx
- AlsalehetalSupplementaryTable4.docx
- AlsalehetalSpdtrialNatureAgingSupplementaryFigureLegends20122024.docx
- AlsalehetalSupplementFiguresNatureAging20122024.pdf